LETTER

doi:10.1038/nature09820

Amygdala circuitry mediating reversible and bidirectional control of anxiety

Kay M. Tye[1]*, Rohit Prakash[1,2]*, Sung-Yon Kim[1,2]*, Lief E. Fenno[1,2]*, Logan Grosenick[1,2], Hosniya Zarabi[1], Kimberly R. Thompson[1], Viviana Gradinaru[1,2], Charu Ramakrishnan[1] & Karl Deisseroth[1,2,3,4,5]

Anxiety—a sustained state of heightened apprehension in the absence of immediate threat—becomes severely debilitating in disease states[1]. Anxiety disorders represent the most common of psychiatric diseases (28% lifetime prevalence)[2] and contribute to the aetiology of major depression and substance abuse[3,4]. Although it has been proposed that the amygdala, a brain region important for emotional processing[5–8], has a role in anxiety[9–13], the neural mechanisms that control anxiety remain unclear. Here we explore the neural circuits underlying anxiety-related behaviours by using optogenetics with two-photon microscopy, anxiety assays in freely moving mice, and electrophysiology. With the capability of optogenetics[14–16] to control not only cell types but also specific connections between cells, we observed that temporally precise optogenetic stimulation of basolateral amygdala (BLA) terminals in the central nucleus of the amygdala (CeA)—achieved by viral transduction of the BLA with a codon-optimized channelrhodopsin followed by restricted illumination in the downstream CeA—exerted an acute, reversible anxiolytic effect. Conversely, selective optogenetic inhibition of the same projection with a third-generation halorhodopsin[15] (eNpHR3.0) increased anxiety-related behaviours. Importantly, these effects were not observed with direct optogenetic control of BLA somata, possibly owing to recruitment of antagonistic downstream structures. Together, these results implicate specific BLA–CeA projections as critical circuit elements for acute anxiety control in the mammalian brain, and demonstrate the importance of optogenetically targeting defined projections, beyond simply targeting cell types, in the study of circuit function relevant to neuropsychiatric disease.

Despite the high prevalence[1,2] of anxiety disorders, the underlying neural circuitry is incompletely understood. Available treatments are inconsistently effective or, in the case of benzodiazepines, addictive and linked to significant side effects including cognitive impairment and respiratory suppression[17], pointing to the need for a deeper understanding of anxiety control mechanisms in the mammalian brain.

Although amygdala microcircuitry for conditioned fear has been optogenetically dissected[18,19], the causal underpinnings of unconditioned anxiety[11] have not yet been investigated with cellular precision. Pointing to the need for precise optogenetic exploration, the amygdala is composed of functionally and morphologically heterogeneous subnuclei with complex interconnectivity. The BLA is primarily glutamatergic (~90%)[20,21] whereas the CeA, which encompasses the centrolateral (CeL) and centromedial (CeM) nuclei, consists of ~95% GABAergic medium spiny neurons[22]. The primary output region of the amygdala is the CeM[23,24], which (when chemically or electrically excited) mediates autonomic and behavioural responses associated with fear and anxiety via projections to the brainstem[25]. Because patients with generalized anxiety disorder may have abnormal activity arising from the BLA and CeM[11], and as BLA neurons excite GABAergic CeL neurons[26] that provide feed-forward inhibition onto CeM 'output' neurons[6,18], we considered that the BLA–CeL–CeM circuitry could be causally involved in anxiety. However, BLA pyramidal neurons as a whole could have varied and antagonistic roles in diverse projections throughout the brain, with targets including the bed nucleus of the stria terminalis (BNST), nucleus accumbens, hippocampus and cortex[26].

We therefore developed a method to selectively control BLA terminals in the CeA (Supplementary Methods). BLA glutamatergic projection neurons were transduced with an adeno-associated virus serotype 5 (AAV_5) carrying codon-optimized channelrhodopsin (ChR2)–eYFP under control of the CaMKIIα promoter followed by unilateral implantation of a bevelled guide cannula to allow preferential illumination of the non-transduced CeL (Supplementary Figs 1, 2). *In vivo* electrophysiological recordings were used to determine illumination parameters for selective control of those BLA terminals in the CeA without nonspecific control of all BLA somata (Supplementary Fig. 3).

To investigate the functional role of the BLA–CeA pathway in anxiety, we probed freely moving mice under projection-specific optogenetic control in two well-validated[27] anxiety assays: the elevated-plus maze (EPM) and the open-field test (OFT) (Fig. 1a–e). Mice display anxiety-related behaviours in open spaces; therefore, increased time spent in the open arms of the EPM or in the centre of the OFT is interpreted as reduced anxiety[27]. To test whether anxiety-related behaviours could be related to activation of the BLA–CeA projection, and not all BLA somata as a whole, we compared mice receiving projection-specific photostimulation (ChR2:BLA–CeA; Fig. 1a) to a group with identical illumination parameters transduced with a control virus (eYFP:BLA–CeA), and to another control group expressing ChR2 in the BLA receiving direct illumination of the BLA (ChR2:BLA(somata)). Photostimulation of BLA terminals in the CeA (ChR2:BLA–CeA) increased open-arm time ($F_{1,42} = 69.09$, $P < 0.00001$; Fig. 1b, c) and the probability of open-arm entry from the maze centre ($F_{1,42} = 24.69$, $P < 0.00001$; Fig. 1c, inset, and Supplementary Movie) on the EPM, as well as increasing centre time in the OFT ($F_{1,105} = 24.46$, $P < 0.00001$; Fig. 1d, e), reflecting anxiety reduction without impaired locomotion (Supplementary Fig. 4). In contrast, the ChR2:BLA(somata) group showed reduced open-arm time ($F_{1,42} = 6.20$, $P = 0.02$; Fig. 1b, c) and probability of open-arm entry ($F_{1,42} = 5.15$, $P = 0.03$) during photostimulation relative to eYFP:BLA–CeA controls, reflecting a distinct anxiogenic effect. Thus, selective illumination of BLA projections to the CeA, but not of BLA somata nonspecifically, produced an acute, rapidly reversible anxiolytic effect.

Next we investigated the physiological basis of this light-induced anxiolysis. We considered that preferential photostimulation of BLA terminals in the CeL could activate CeL neurons and exert feed-forward inhibition onto brainstem-projecting CeM output neurons[18] to implement anxiolysis. To test this, we undertook *in vivo* experiments, with light-delivery protocols matched to those delivered in the behavioural experiments, using activity-dependent immediate early

[1]Department of Bioengineering, Stanford University, Stanford, California 94305, USA. [2]Neurosciences Program, Stanford University, Stanford, California 94305, USA. [3]Department of Psychiatry and Behavioral Sciences, Stanford University, Stanford, California 94305, USA. [4]Howard Hughes Medical Institute, Stanford University, Stanford, California 94305, USA. [5]CNC Program, Stanford University, Stanford, California 94305, USA.
*These authors contributed equally to this work.

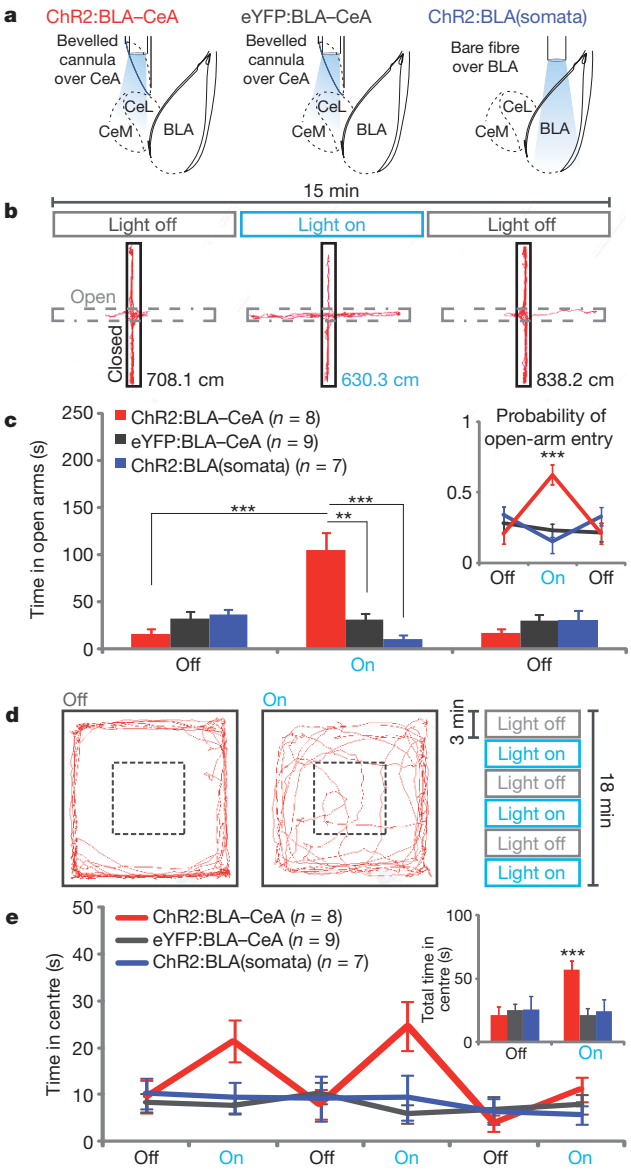

Figure 1 | Projection-specific excitation of BLA terminals in the CeA induces acute reversible anxiolysis. **a**, Mice were housed in a high-stress environment before behavioural manipulations, and received 5-ms light pulses at 20 Hz for all light-on conditions. **b**, **c**, ChR2:BLA–CeA mice ($n = 8$) received selective illumination of BLA terminals in the CeA during the light-on epoch on the EPM; see ChR2:BLA–CeA representative path (**b**), which induced an increase in open-arm time on photostimulation relative to eYFP:BLA–CeA ($n = 9$) and ChR2:BLA(somata) ($n = 7$) controls (**c**), and an increase in the probability of open-arm entry (see inset). **d**, **e**, ChR2:BLA–CeA mice also showed increased centre time on the OFT, as seen in a representative path (**d**), during light-on epochs relative to light-off epochs and eYFP:BLA–CeA and ChR2:BLA(somata) controls (**e**).

gene (c-*fos*) expression to track neuronal activation. We quantified the proportion of neurons in the BLA, CeL and CeM (Supplementary Fig. 5) within each group that expressed eYFP or showed c-*fos* immunoreactivity. Opsin expression was specific to BLA glutamatergic neurons, and was not observed in intercalated cells (Supplementary Fig. 6). No group differences were detected in the proportion of eYFP-positive cells within each region (Supplementary Fig. 5). We found a significantly higher proportion of c-*fos*-positive BLA cells in the ChR2:BLA(somata) group ($F_{2,9} = 10.12$, $P < 0.01$), relative to the ChR2:BLA–CeA or eYFP:BLA–CeA groups ($P < 0.01$ and $P < 0.05$, respectively), but no detectable difference between the ChR2:BLA–CeA and eYFP:BLA–CeA groups, indicating that the bevelled cannula shielding effectively prevented BLA somata photostimulation. A higher proportion of CeL neurons expressed c-*fos* in the ChR2:BLA–CeA group relative to the eYFP:BLA–CeA group ($F_{2,9} = 4.54$, $P = 0.04$), but not the ChR2:BLA(somata) group (Supplementary Fig. 5). Thus, the *in vivo* illumination of BLA–CeA projections that triggered acute anxiolysis was found to excite CeL neurons without activating BLA somata.

To test the hypothesis that preferential illumination of BLA–CeL terminals induced feed-forward inhibition of CeM output neurons, we combined whole-cell patch-clamp electrophysiology with two-photon imaging to visualize the microcircuit while simultaneously probing the functional relationships among these cells during projection-specific optogenetic control (Fig. 2a–f). BLA neurons showed high-fidelity spiking to direct illumination (Fig. 2b). Illumination of BLA terminals in CeL elicited excitatory responses with stable spiking fidelity, and responding cells included both weakly and strongly excited CeL cells ($n = 16$; Fig. 2c).

To test whether illumination of BLA–CeL synapses could block CeM spiking via feed-forward inhibition from CeL neurons, we recorded from CeM neurons while selectively illuminating BLA–CeL synapses (Fig. 2d). Indeed, we observed potent spiking inhibition in CeM cells on illumination of BLA–CeL terminals (Fig. 2d; $F_{2,11} = 15.35$, $P = 0.004$). Figure 2e shows CeM responses recorded during illumination of ChR2-expressing BLA neurons in the CeM; importantly, the very same CeM neurons ($n = 7$) showed net excitation with broad illumination of BLA inputs to the CeM (Fig. 2e), but showed net inhibition on selective illumination of BLA inputs to the CeL (Fig. 2f). These data from a structurally and functionally identified microcircuit[25] illustrate that the balance of direct and indirect inputs from the BLA to the CeM can modulate CeM activity. We then directly tested whether overlapping or distinct populations of BLA neurons projected to the CeL and CeM in the mouse (Supplementary Fig. 7) by two-photon imaging in 350-μm-thick coronal slices. Of the BLA neurons sampled ($n = 18$; Supplementary Fig. 7), 44% projected to the CeL alone and 17% projected to the CeM alone, with only one cell observed to project to both the CeL and the CeM.

Because *in vivo* c-*fos* assays had indicated that illumination of BLA terminals in the CeL sufficed to drive excitation of postsynaptic CeL neurons but not to recruit efficiently BLA neurons as a whole, we next investigated the properties of optogenetically driven terminal stimulation in this microcircuit using whole-cell recordings. We first recorded from BLA pyramidal neurons expressing ChR2 and moved a restricted light spot (~125 μm in diameter) in 100-μm steps from the cell soma, both in a direction over the visually identified axon and in a direction where there was no axon collateral, illustrating the spatial properties of light scattering in this circuit (Fig. 3a, b); spiking fidelity in the BLA neuron and evoked inward currents are summarized (Fig. 3a). Next, we found that typical photostimulation parameters drove reliable transmission when delivered to BLA–CeA synapses (assayed with recordings from postsynaptic CeL neurons; Fig. 3b and Supplementary Fig. 8); in contrast, when recording from the BLA somata instead, ~300 μm from the light spot, we did not observe reliable antidromically driven action potential firing (only ~5% reliability) despite use of the very same BLA–CeA synapse illumination conditions that elicited 100% reliable transmitter release from the illuminated terminals and the same cells known to spike robustly in response to somatic illumination (Fig. 3b). These results were consistent with the c-*fos* immunoreactivity and behavioural data (Fig. 1) and held even on bath application of GABA and glutamate receptor antagonists ($n = 7$) to eliminate local circuitry effects. The marked difference between effective synaptic transmission and antidromic spiking fidelity ($P = 0.0039$; Fig. 3b, inset) reveals that optogenetically driven vesicle release can occur in the absence of reliable antidromic drive, a potentially useful property that may relate to projection parameters such as axon calibre and myelination status (optogenetic stimuli will recruit thinner axons more efficiently than electrical stimuli), as well as experimental light intensity and spatial restriction properties.

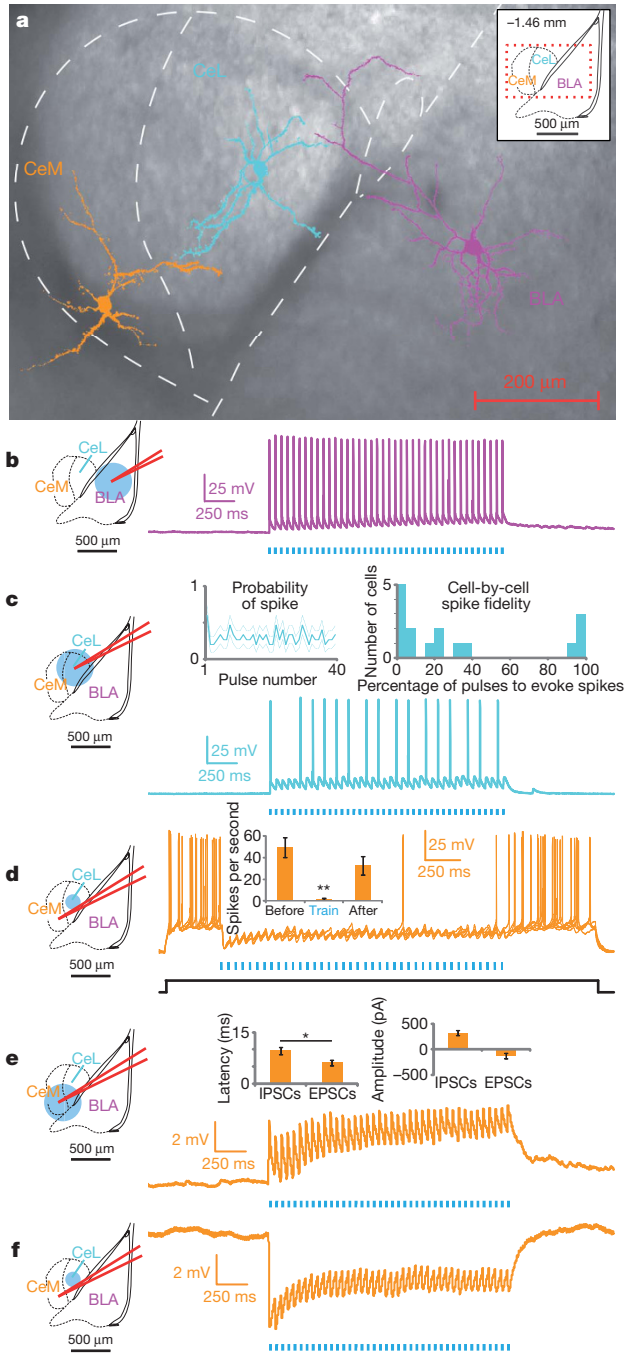

Figure 2 | Projection-specific excitation of BLA terminals in the CeA activates CeL neurons and elicits feed-forward inhibition of CeM neurons. **a**, Two-photon images of representative BLA, CeL and CeM cells imaged from the same slice, overlaid on a brightfield image. **b**–**f**, Schematics of the recording and illumination sites for the associated representative current-clamp traces (membrane potential $V_m = \sim -70$ mV). **b**, Representative BLA pyramidal neuron trace expressing ChR2, all of which spiked for every pulse ($n = 4$). **c**, Representative trace from a CeL neuron in the terminal field of BLA projection neurons, showing both sub- and suprathreshold excitatory responses on photostimulation ($n = 16$). Inset left, population summary of mean probability of spiking for each pulse in a 40-pulse train at 20 Hz, dotted lines indicate s.e.m. Inset right, frequency histogram showing individual cell spiking fidelity; *y*-axis is the number of cells per each 5% bin. **d**, Six sweeps from a CeM neuron spiking in response to a current step (~60 pA; indicated in black) and inhibition of spiking on 20 Hz illumination of BLA terminals in the CeL. Inset, spike frequency was significantly reduced during light stimulation of CeL neurons ($n = 4$; spikes per second before (49 ± 9.0), during (1.5 ± 0.87) and after (33 ± 8.4) illumination; mean ± s.e.m.). **e**, **f**, On broad illumination of the CeM, voltage-clamp summaries show that the latency of excitatory postsynaptic currents (EPSCs) is significantly shorter than the latency of inhibitory postsynaptic currents (IPSCs), whereas there was a non-significant difference in the amplitude of EPSCs and IPSCs ($n = 11$; $^*P = 0.04$, see insets). The same CeM neurons ($n = 7$) showed either net excitation when receiving illumination of the CeM (**e**) or net inhibition on selective illumination of the CeL (**f**).

To confirm further that the anxiolytic effect was due to the selective activation of BLA–CeL projections alone, and not BLA axons passing through the CeA or back-propagation of action potentials to BLA cell bodies that would then innervate all BLA projection target regions, we tested whether local glutamate receptor antagonism would attenuate light-induced anxiolytic effects. This distinction is critical, as there have been previous reports that CeA lesions that alter anxiety are confounded by the ablation of BLA projections to the BNST passing through the CeA[28]. In a separate group of mice, we selectively illuminated BLA–CeA terminals as before ($n = 8$; Supplementary Fig. 1), but infused glutamate antagonists or saline via the fibre-optic guide cannula before testing on the EPM and OFT. Confirming a local synaptic mechanism rather than control of fibres of passage, intra-CeA glutamate receptor antagonism abolished light-induced reductions in anxiety as measured by open-arm time ($F_{1,35} = 8.61$, $P = 0.008$) and probability of open-arm entry on the EPM ($F_{1,35} = 5.92$, $P = 0.02$), and centre time during the OFT ($F_{1,77} = 13.99$, $P = 0.0006$; Fig. 3c, d). Importantly, drug treatment did not impair locomotor activity (Supplementary Fig. 9), and in acute slices time-locked light-evoked excitatory responses were abolished on bath application of 2,3-dihydroxy-6-nitro-7-sulfamoyl-benzo[f]quinoxaline-2,3-dione (NBQX) and (2R)-amino-5-phosphonovaleric acid; (2R)-amino-5-phosphonopentanoate (AP5) (Supplementary Fig. 10). These data demonstrate that the light-induced anxiolytic effects were caused by the activation of BLA–CeA synapses, and not attributable to BLA projections to distal targets passing through the CeA.

Finally, to test whether basal anxiety-reducing processes could be blocked by selectively inhibiting the BLA–CeA pathway, we bilaterally transduced either eNpHR3.0—which hyperpolarizes neuronal membranes on illumination with amber light[15]—or eYFP alone, under the CaMKIIα promoter in the BLA, and implanted bilateral bevelled guide cannulae to allow selective illumination of BLA terminals in the CeA (Supplementary Fig. 11). eNpHR3.0 expression was restricted to glutamatergic neurons in the BLA, and the eNpHR3.0:BLA–CeA group showed raised levels of c-*fos* expression relative to the eYFP:BLA–CeA and eNpHR3.0:BLA(somata) groups in the CeM ($P < 0.05$; Supplementary Fig. 12), consistent with the hypothesis that inhibition of BLA–CeL synapses suppresses feed-forward inhibition from CeL neurons to CeM neurons, thereby increasing CeM excitability and the downstream processes leading to increased anxiety phenotypes. Selective illumination of eNpHR3.0-expressing axon terminals reduced the probability of both spontaneously occurring (frequency: $F_{1,8} = 32.99$, $P = 0.00024$; amplitude: $F_{1,8} = 21.96$, $P = 0.001$; Supplementary Fig. 13) and electrically evoked ($F_{1,10} = 10.79$, $P = 0.006$; Fig. 4a) vesicle release, without preventing spiking at the soma (Supplementary Fig. 14). BLA somata inhibition did not induce an anxiogenic response, perhaps owing to the simultaneous decrease in direct BLA–CeM excitatory input. We also found that the eNpHR3.0:BLA–CeA group showed reduced open-arm time and probability of open-arm entry on the EPM ($F_{1,40} = 21.08$, $P < 0.00001$; and $F_{1,40} = 19.93$, $P < 0.00001$, respectively; Fig. 4b, c) and centre time in the OFT ($F_{1,100} = 18.919$, $P < 0.00001$; Fig. 4d, e) during photostimulation when compared to the eYFP and BLA(somata) groups, without altering locomotor activity (Supplementary Fig. 15). These data demonstrate that preferential inhibition of BLA–CeL synapses acutely increases anxiety-like behaviours.

Here, we have identified the BLA–CeL pathway as a neural substrate for real-time bidirectional modulation of the unconditioned expression of anxiety. The observation that selective illumination of specific BLA terminals produces distinct, and even opposite, behavioural responses

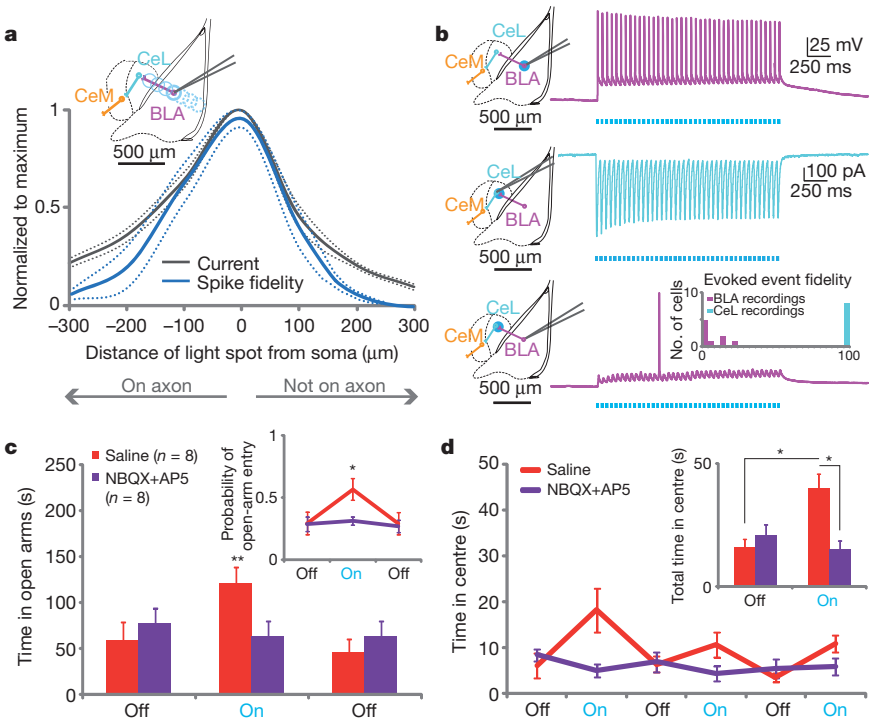

Figure 3 | Light-induced anxiolytic effects are attributable to activation of BLA–CeA synapses. **a**, **b**, Schematic of the recording site and illumination positions as whole-cell recordings were performed at each illumination location in 100-µm increments away from the cell soma both over a visualized axon and in a direction that was not over an axon (inset). Normalized summary of spike fidelity and depolarizing current (**a**) to a 20-Hz train delivered at various distances from the soma. **b**, Representative traces on ~125-µm-diameter illumination at various locations within each slice ($n = 7$). Illumination of BLA somata elicits high-fidelity spiking (top). Illumination of BLA terminals in CeL elicits strong excitatory responses shown in voltage-clamp in the postsynaptic CeL neuron (middle), but does not elicit reliable antidromic spiking in the BLA neuron itself (bottom), summarized in a frequency histogram (inset, 120 pulses per cell). **c**, **d**, A separate group of ChR2:BLA–CeA mice ($n = 8$) performed the EPM and OFT twice, one session preceded with intra-CeA infusions of saline (red) and the other session with glutamate receptor antagonists NBQX and AP5 (purple), counter-balanced for order. Glutamate receptor blockade in the CeA attenuated light-induced increases in both open-arm time (**c**) and probability of open-arm entry (inset) on the EPM and centre time on the OFT (**d**, inset shows pooled summary), without altering baseline performance.

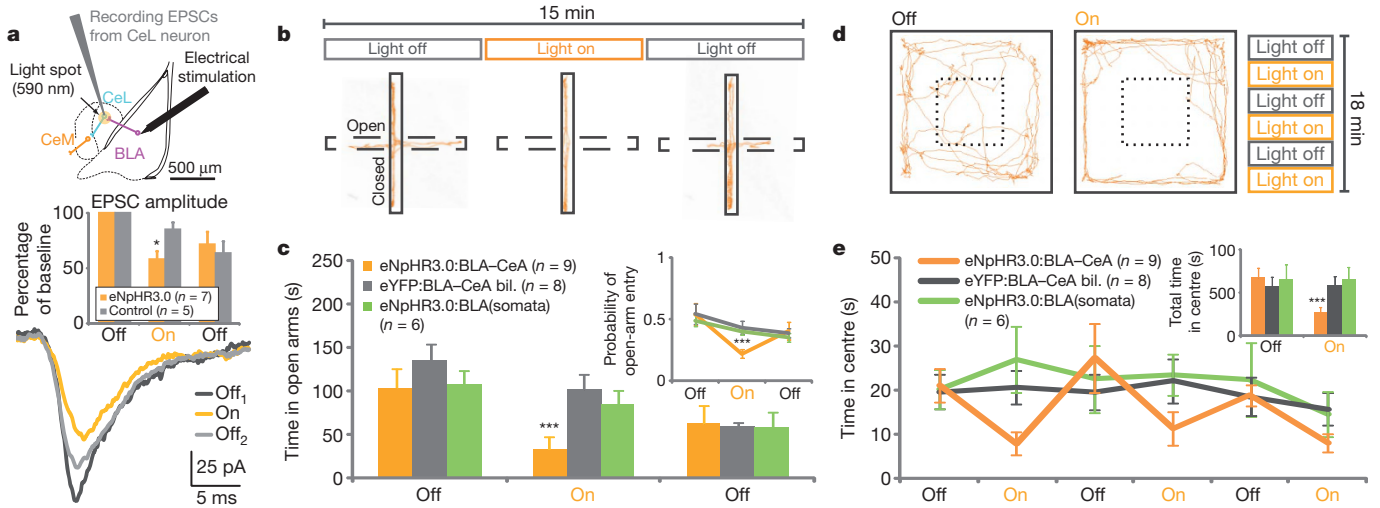

Figure 4 | Selective inhibition of BLA terminals in the CeA induces an acute and reversible increase in anxiety. **a**–**e**, Mice were group-housed in a low-stress environment and received bilateral constant 594-nm light during light-on epochs. **a**, Selective illumination of eNpHR3.0-expressing BLA terminals suppresses vesicle release evoked by electrical stimulation in the BLA. Schematic indicates the locations of the stimulating electrode, the recording electrode and the ~125-µm diameter light spot. Representative CeL EPSCs before (Off_1), during (On) and after (Off_2) selective illumination of eNpHR3.0-expressing BLA terminals. Normalized EPSC amplitude summary data from sections containing BLA neurons expressing eNpHR3.0 ($n = 7$) and non-transduced controls ($n = 5$) show that selectively illuminating BLA–CeL terminals reduces ($^*P = 0.006$) electrically evoked EPSC amplitude in postsynaptic CeL neurons relative to non-transduced control slice preparations (inset). **b**, **c**, Representative eNpHR3.0:BLA–CeA path (**b**) indicates reduced open-arm time (**c**) and probability of open arm entry (inset) during illumination, relative to controls. bil., bilateral. **d**, **e**, Representative eNpHR3.0:BLA–CeA path (**d**) reflects reduced centre time on the OFT (**e**) for the eNpHR3.0:BLA–CeA group during light-on, but not light-off, epochs as compared to controls (inset shows pooled data).

from illumination of all glutamatergic BLA somata nonspecifically, points to the essential value of optogenetic control in causally dissecting intact neural circuitry, and indicates that multiple subpopulations or projections of BLA neurons can act in opposition (for example, direct excitation of CeM along with feed-forward inhibition of CeM). Neural circuitry arranged in this way provides many opportunities for modulation of expression of anxiety phenotypes; for example, this microcircuit is well-positioned to be influenced by top-down cortical control from regions important for processing fear and anxiety, including the prelimbic, infralimbic, anterior cingulate and insular cortices that provide robust innervation to the BLA and CeL.

These data are consistent with reports implicating CeA involvement in anxiety[9,11,12], but it is important to note that our findings do not exclude downstream or parallel circuits including the BNST[28], the insular and prefrontal cortices[29], and the septal–hippocampal circuit[30]; for example, stress induces CeL release of corticotropin releasing hormone (CRH) in the BNST[28]. In the course of providing insight into native anxiogenic and anxiolytic processes, these findings demonstrate that anxiety is continuously regulated by balanced antagonistic pathways within the amygdala, and illustrate the importance of resolving specific projections in the study of neural circuit function relevant to psychiatric disease.

METHODS SUMMARY

Virus-mediated opsin gene expression. The pAAV-CaMKIIα-hChR2(H134R)-eYFP, pAAV-CaMKIIα-eYFP and pAAV-CaMKIIα-eNpHR3.0-eYFP plasmids were designed and constructed by standard methods and packaged as AAV_5. Virus (0.5 μl) was injected into the BLA. Maps and clones are available at http://www.optogenetics.org.

***In vivo* projection-specific targeting.** To investigate the role of the BLA–CeL pathway in modulating anxiety, we performed viral transduction and surgical implantation of bevelled guide cannulae to allow selective illumination of BLA fibres in the CeA under stereotaxic guidance. Behavioural, electrophysiological and imaging data were collected 4–6 weeks after surgery.

Two-photon imaging and functional mapping using *ex vivo* electrophysiology. Acute slices were collected for two-photon imaging and *ex vivo* electrophysiological recordings. While light-stimulation parameters used *in vivo* were delivered via fibre optics, and light in *ex vivo* experiments was delivered onto coronal sections, we matched light power density at our target region $\sim 6\ mW\ mm^{-2}$. Whole-cell recordings were made from BLA pyramidal neurons simultaneously during two-photon visualization of neuronal processes with Alexa Fluor dye. We visually tracked axonal projections from BLA neurons to the CeL nucleus. We recorded from CeL neurons on illumination with an aperture-restricted light spot ($\sim$125 μm diameter), mimicking the preferential illumination of BLA terminals, but not BLA somata, delivered *in vivo*. Two-photon imaging allowed axonal tracking to the CeM, where whole-cell recordings were collected from CeM neurons in the terminal field of CeL axons, with aperture-restricted illumination over the CeL to allow selective illumination of BLA terminals in the CeL while recording from the CeM neuron.

Opsin expression validation and immunohistochemistry. To validate specificity, sensitivity and spatial distribution of opsin expression as well as neuronal activity, brain slices were prepared for optical microscopy and immunohistochemistry. Coronal sections were stained for 4′,6-diamidino-2-phenylindole (DAPI) and immunoreactivity for c-*fos*. Quantitative analyses of confocal images were performed with both staining and analysis blind to experimental condition.

Received 7 November 2010; accepted 14 January 2011.
Published online 9 March 2011.

1. Lieb, R. Anxiety disorders: clinical presentation and epidemiology. *Handb. Exp. Pharmacol.* **169,** 405–432 (2005).
2. Kessler, R. C. *et al.* Lifetime prevalence and age-of-onset distributions of DSM-IV disorders in the National Comorbidity Survey Replication. *Arch. Gen. Psychiatry* **62,** 593–602 (2005).
3. Koob, G. F. Brain stress systems in the amygdala and addiction. *Brain Res.* **1293,** 61–75 (2009).
4. Ressler, K. J. & Mayberg, H. S. Targeting abnormal neural circuits in mood and anxiety disorders: from the laboratory to the clinic. *Nature Neurosci.* **10,** 1116–1124 (2007).
5. LeDoux, J. The emotional brain, fear, and the amygdala. *Cell. Mol. Neurobiol.* **23,** 727–738 (2003).
6. Pare, D., Quirk, G. J. & Ledoux, J. E. New vistas on amygdala networks in conditioned fear. *J. Neurophysiol.* **92,** 1–9 (2004).
7. Tye, K. M., Stuber, G. D., de Ridder, B., Bonci, A. & Janak, P. H. Rapid strengthening of thalamo-amygdala synapses mediates cue–reward learning. *Nature* **453,** 1253–1257 (2008).
8. Weiskrantz, L. Behavioral changes associated with ablation of the amygdaloid complex in monkeys. *J. Comp. Physiol. Psychol.* **49,** 381–391 (1956).
9. Kalin, N. H., Shelton, S. E. & Davidson, R. J. The role of the central nucleus of the amygdala in mediating fear and anxiety in the primate. *J. Neurosci.* **24,** 5506–5515 (2004).
10. Lesscher, H. M. *et al.* Amygdala protein kinase C epsilon regulates corticotropin-releasing factor and anxiety-like behavior. *Genes Brain Behav.* **7,** 323–333 (2008).
11. Etkin, A., Prater, K. E., Schatzberg, A. F., Menon, V. & Greicius, M. D. Disrupted amygdalar subregion functional connectivity and evidence of a compensatory network in generalized anxiety disorder. *Arch. Gen. Psychiatry* **66,** 1361–1372 (2009).
12. Lyons, A. M. & Thiele, T. E. Neuropeptide Y conjugated to saporin alters anxiety-like behavior when injected into the central nucleus of the amygdala or basomedial hypothalamus in BALB/cJ mice. *Peptides* **31,** 2193–2199 (2010).
13. Roozendaal, B., McEwen, B. S. & Chattarji, S. Stress, memory and the amygdala. *Nature Rev. Neurosci.* **10,** 423–433 (2009).
14. Boyden, E. S., Zhang, F., Bamberg, E., Nagel, G. & Deisseroth, K. Millisecond-timescale, genetically targeted optical control of neural activity. *Nature Neurosci.* **8,** 1263–1268 (2005).
15. Gradinaru, V. *et al.* Molecular and cellular approaches for diversifying and extending optogenetics. *Cell* **141,** 154–165 (2010).
16. Deisseroth, K. Optogenetics: controlling the brain with light. *Sci. Am.* **303,** 48–55 (2010).
17. Woods, J. H., Katz, J. L. & Winger, G. Benzodiazepines: use, abuse, and consequences. *Pharmacol. Rev.* **44,** 151–347 (1992).
18. Ciocchi, S. *et al.* Encoding of conditioned fear in central amygdala inhibitory circuits. *Nature* **468,** 277–282 (2010).
19. Haubensak, W. *et al.* Genetic dissection of an amygdala microcircuit that gates conditioned fear. *Nature* **468,** 270–276 (2010).
20. Carlsen, J. Immunocytochemical localization of glutamate decarboxylase in the rat basolateral amygdaloid nucleus, with special reference to GABAergic innervation of amygdalostriatal projection neurons. *J. Comp. Neurol.* **273,** 513–526 (1988).
21. Smith, Y. & Pare, D. Intra-amygdaloid projections of the lateral nucleus in the cat: PHA-L anterograde labeling combined with postembedding GABA and glutamate immunocytochemistry. *J. Comp. Neurol.* **342,** 232–248 (1994).
22. McDonald, A. J. Cytoarchitecture of the central amygdaloid nucleus of the rat. *J. Comp. Neurol.* **208,** 401–418 (1982).
23. Krettek, J. E. & Price, J. L. A description of the amygdaloid complex in the rat and cat with observations on intra-amygdaloid axonal connections. *J. Comp. Neurol.* **178,** 255–279 (1978).
24. Krettek, J. E. & Price, J. L. Amygdaloid projections to subcortical structures within the basal forebrain and brainstem in the rat and cat. *J. Comp. Neurol.* **178,** 225–253 (1978).
25. Davis, M. in *The Amygdala: A Functional Analysis* (ed. Aggleton, J. P.) 213–288 (Oxford Univ. Press, 2000).
26. Pitkanen, A. in *The Amygdala: A Functional Analysis* (ed. Aggleton, J. P.) 31–99 (Oxford Univ. Press, 2000).
27. Carola, V., D'Olimpio, F., Brunamonti, E., Mangia, F. & Renzi, P. Evaluation of the elevated plus-maze and open-field tests for the assessment of anxiety-related behaviour in inbred mice. *Behav. Brain Res.* **134,** 49–57 (2002).
28. Davis, M., Walker, D. L., Miles, L. & Grillon, C. Phasic vs sustained fear in rats and humans: role of the extended amygdala in fear vs anxiety. *Neuropsychopharmacology* **35,** 105–135 (2010).
29. Shin, L. M. & Liberzon, I. The neurocircuitry of fear, stress, and anxiety disorders. *Neuropsychopharmacology* **35,** 169–191 (2010).
30. Gray, J. A. & McNaughton, N. The neuropsychology of anxiety: reprise. *Nebr. Symp. Motiv.* **43,** 61–134 (1996).

Supplementary Information is linked to the online version of the paper at www.nature.com/nature.

Acknowledgements We would like to thank P. Janak, H. Fields, G. Stuber, E. Thomas, F. Zhang, I. Witten, V. Sohal, T. Davidson and M. Warden as well as J. Mattis, R. Durand, M. Mogri, J. Mirzabekov and E. Steinberg for discussions, and the entire K.D. laboratory for their support. All viruses were packaged at University of North Carolina (UNC) Vector Core. Supported by NIMH (1F32MH088010-01, K.M.T.), NARSAD (K.R.T.), Samsung Scholarship (S.-Y.K.), NSF IGERT Award 0801700 (L.G.) and the Defense Advanced Research Projects Agency Reorganization and Plasticity to Accelerate Injury Recovery (N66001-10-C-2010), the Alice Woo, Albert Yu, Snyder, and McKnight Foundations, as well as NIDA, NIMH and the NIH Pioneer Award (K.D.)

Author Contributions K.M.T., R.P., S.-Y.K., L.E.F. and K.D. contributed to study design and data interpretation. K.M.T., R.P., S.-Y.K. and L.E.F. contributed to data collection and K.M.T. coordinated data collection and analysis. K.M.T., S.-Y.K., H.Z. and K.R.T. contributed to immunohistochemical processing, fluorescence imaging and quantitative analyses. K.M.T. and L.G. performed the behavioural and *ex vivo* electrophysiology statistical analyses. V.G. and C.R. contributed to the design of eNpHR3.0. C.R. cloned all constructs and managed viral packaging processes. K.D. supervised all aspects of the work. All authors contributed to writing the paper.

Author Information Reprints and permissions information is available at www.nature.com/reprints. The authors declare no competing financial interests. Readers are welcome to comment on the online version of this article at www.nature.com/nature. Correspondence and requests for materials should be addressed to K.D. (deissero@stanford.edu).